

Colliding nuclei to colliding galaxies: Illustrations using a simple colliding liquid-drop apparatus

F. D. Becchetti, S. L. Mack, W. R. Robinson, and M. Ojaruega

Citation: *American Journal of Physics* **83**, 846 (2015); doi: 10.1119/1.4926958

View online: <http://dx.doi.org/10.1119/1.4926958>

View Table of Contents: <http://scitation.aip.org/content/aapt/journal/ajp/83/10?ver=pdfcov>

Published by the [American Association of Physics Teachers](#)

Articles you may be interested in

[Comparative Cognitive Task Analyses of Experimental Science and Instructional Laboratory Courses](#)

Phys. Teach. **53**, 349 (2015); 10.1119/1.4928349

[Bouncing Back From “Deflategate”](#)

Phys. Teach. **53**, 341 (2015); 10.1119/1.4928347

[Report: AAPT Recommendations for the Undergraduate Physics Laboratory Curriculum](#)

Phys. Teach. **53**, 253 (2015); 10.1119/1.4914580

[The ‘Nut-Drop’ Experiment—Bringing Millikan’s Challenge to Introductory Students](#)

Phys. Teach. **47**, 374 (2009); 10.1119/1.3204120

[Planets and Galaxies on Soap Films](#)

Phys. Teach. **44**, 392 (2006); 10.1119/1.2336150



American Association of **Physics Teachers**

Explore the **AAPT Career Center** – access hundreds of physics education and other STEM teaching jobs at two-year and four-year colleges and universities.

<http://jobs.aapt.org>



Colliding nuclei to colliding galaxies: Illustrations using a simple colliding liquid-drop apparatus

F. D. Becchetti,^{a)} S. L. Mack,^{b)} W. R. Robinson,^{c)} and M. Ojaruega^{d)}
Department of Physics, University of Michigan, Ann Arbor, Michigan 48109-1040

(Received 5 August 2011; accepted 3 July 2015)

A simple apparatus suitable for observing the collisions between drops of fluids of various properties is described. Typical results are shown for experiments performed by undergraduate students using various types of fluids. The collisions take place under free-fall (zero-*g*) conditions, with analysis employing digital video. Two specific types of collisions are examined in detail, head-on collisions and peripheral, grazing collisions. The collisions for certain fluids illustrate many types of nuclear collisions and provide useful insight into these processes, including both fusion and non-fusion outcomes, often with the formation of exotic shapes or emission of secondary fragments. Collisions of other liquids show a more chaotic behavior, often resembling galactic collisions. As expected, the Weber number associated with a specific collision impact parameter is found to be the important quantity in determining the initial outcome of these colliding systems. The features observed resemble those reported by others using more elaborate experimental techniques. © 2015 American Association of Physics Teachers.

[<http://dx.doi.org/10.1119/1.4926958>]

I. INTRODUCTION

Most people would consider a leaky, dripping faucet to be an annoyance. However, careful observation (using, for example, stroboscopic techniques^{1,2}) reveals a fascinating world of exotic shapes controlled by the physics of fluid dynamics. The classic stroboscopic picture of milk drops splashing into a cup of coffee is a well-known example of such phenomena.^{2,3} The basic necking process which forms the drop emerging from a faucet or orifice is non-trivial and differs from most expectations.^{4,5} Likewise, drop oscillations and the collision of drops (e.g., rain drops) can also reveal unexpected characteristics including unusual necking, bridging, extended shapes, and specific types of fragmentation.⁶⁻⁹ In order to reduce the effects of gravity, many of the experiments involving the study of liquids have used NASA's free-fall towers or were done in orbiting spaceships by astronauts.¹⁰

Observations of colliding liquid drops can be used to provide students with insight into a wide variety of multi-particle colliding systems, ranging from colliding nuclei to colliding galaxies. The wide range of experiments possible with this type of apparatus can provide (and have provided) motivation for students to pursue more detailed studies of fluids as well as the related nuclear and astrophysical processes that can be illustrated with such apparatus. As an example of the latter, one of the earliest models of the nucleus, the nuclear liquid drop model (LDM), was first posited by von Weizsacker in 1935¹¹ and refined by Bohr in 1936,¹² considers the nucleus to be well represented by a non-compressible fluid¹³ or a fluid that maintains a constant volume when its shape is changed (such as a liquid drop). Many fluids such as water and oil behave like this.

The development of the LDM was based on three features of the nucleus: the constant average binding energy per nucleon, the nearly constant central nuclear density, and the presence of strong surface-tension effects. At high values of internal excitation energy, microscopic nuclear pairing effects and nuclear shell effects are expected to vanish. Thus, a macroscopic model of a non-compressible fluid such as the LDM can provide a surprisingly accurate

representation of basic nuclear properties, such as nuclear masses and reaction *Q*-values,¹⁴ fusion and fission,¹⁵⁻²⁴ and nucleus-nucleus collisions.²⁵⁻²⁹

Here, we describe an apparatus³⁰ utilizing video capture³¹⁻³⁴ specifically designed to illustrate key features of many types of nuclear and other collisions using various (charged and uncharged) liquids,³⁵ including oil, water, water with glycerine, and water with a wetting agent. Oil drops best represent the conditions found in nuclear collisions, while collisions of other liquids can provide insight into a wide variety of other collisional phenomena, including collisions involving sub-atomic particles, molecules, asteroids, planets, galaxies, and even neutron stars.³⁶⁻⁴⁶

II. DESCRIPTION OF APPARATUS

The apparatus described here has been used by undergraduate students over several years for individual research projects studying various types of collisions, specifically: (1) head-on and grazing collisions between oil drops of equal or unequal size; (2) head-on and grazing collisions between water drops of equal or unequal size; (3) same as (2) but with a wetting agent added to reduce surface tension; (4) same as (1) and (2) but with contrasting color dyes added to the drops; (5) same as (1) and (2) but with high-voltage electrodes added to provide repulsive charges on the drops to better illustrate nuclear collisions.

In place of the more elaborate (and more precise) experimental techniques employed by others, we have developed a simplified apparatus designed for use by undergraduates to study collisions between drops in air in free fall. There are, however, some limitations: (1) knowledge of the mass and size of the drops is less precise; (2) the vertical motion of the drops introduces distortions in the drops' trajectories; (3) the drops may be in an oscillating (i.e., *excited*) state when colliding; and (4) precise analysis of the relative closing velocity and impact parameters is more difficult and hence less precise. Many of the latter difficulties are addressed by introducing stroboscopic, high-speed digital video (DV) techniques to observe and analyze the drop trajectories and

collisions in free fall. Since students are often dealing with simulations of nuclear collisions, the type of analysis described by Menchaca-Rocha *et al.*^{26–28} is employed.

The apparatus allows the addition of a wetting agent or repulsive charges to the drops to alter the features of the collision, while contrasting colored drops enable one to track the flow of matter between the drops as they collide. Two different collision outcomes are expected to exist for colliding drops: coalescence and fragmentation.^{26–28} The boundary between these regimes is a function of the relative closing velocity, impact parameter (i.e., the centrality of the collision), the drops' densities, their viscosities, and the surface tension of the liquids. The apparatus permits the use of a variety of drop sizes, impact parameters, and liquid properties, so that students can investigate the collisions in each of these regimes. In addition, the salient features of each type of collision can be examined, especially the evolution of exotic shapes, the transfer of mass during the collision using colored drops, and the creation of fragmentation residues.

Figure 1 shows the basic setup (not drawn to scale) with relevant physical parameters noted in Fig. 2. This arrangement is based on the “double piddle,” from a design provided to us by the late Professor Crane.³⁰ Liquid drops of nearly equal size and equal mass, or alternately unequal size and mass, are ejected from each nozzle, and follow a trajectory similar to the one indicated in Fig. 1(a). In the basic setup, the liquid is drawn out of a reservoir and driven by a single oscillating pump. The pulsed stream travels from the pump through vinyl tubing and is split into two streams traveling through similar tubing. The streams subsequently go through smaller-diameter tubing and arrive at straight, horizontal nozzles attached to ring stands (see Fig. 1). The latter have X-Y-Z adjustments available using microscope or optical stages attached either to the nozzles or to the ring-stand bases, which are mounted on an optical bench. The individual horizontal velocities and hence the closing velocity of the drops is controlled by the voltage input to the pulsating pump via a variac. The trajectory of the drops shown schematically in Fig. 1(a) closely approximates that of the oil drops. In contrast, the water-based drops that are less massive follow a more horizontal trajectory. The lowest relative collision velocities (or closing velocities) were obtained by having the drops collide at an angle to each other, for example, by setting the nozzles at an angle relative to their nominal parallel orientation. While a laser can initially be used to align the nozzles, observation of the actual drop collisions is the best method for final alignment, especially for variation of the impact parameter b (see below). Drop sizes are controlled by the size of the nozzle used and typically range from 3–8 mm in diameter for the nozzles used here. All liquid-drop residues, except when colored drops are used, are collected in the reservoir and recycled through the pumps.

When the drops are ejected from the nozzles, they are usually still connected to each other in a pulsed stream. As they travel through the air a few, they eventually separate and form distinct, primarily spherical drops. Images of the drops were recorded using a digital video system with a shutter speed of 1/4000 s, and subsequently analyzed using the program NIH Image.³¹ Alternately, commercial video-analysis programs such as VideoPoint³² or Logger PRO³³ can also be used. In most cases, a grid is then inserted close to the collision region to minimize parallax and recorded on DV for calibration purposes. The pump listed in Table I provides a

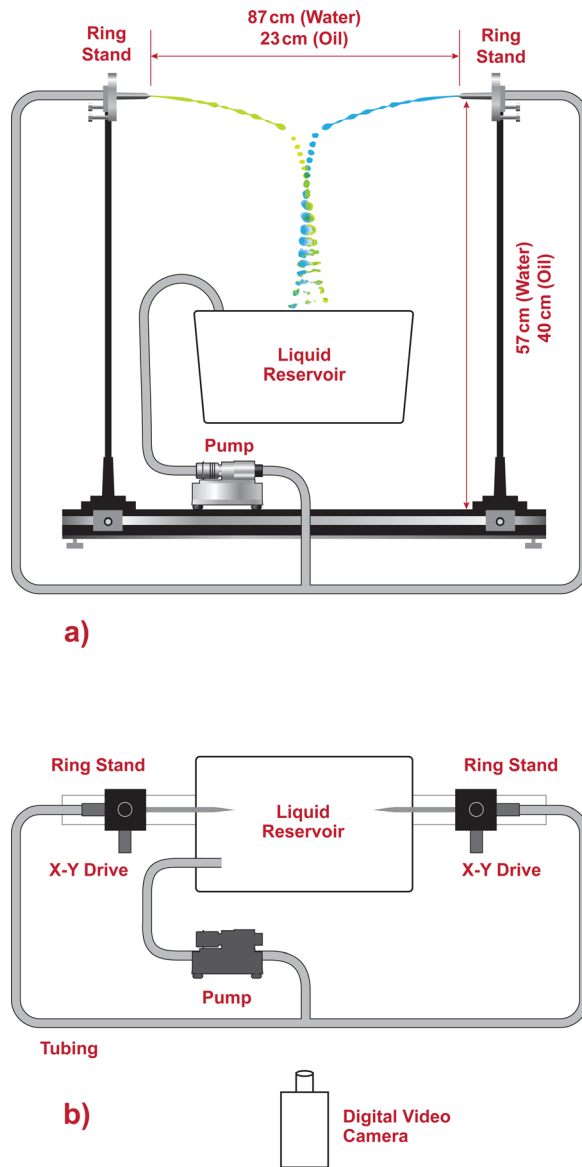


Fig. 1. Schematic diagram of the apparatus setup: (a) side view; (b) overhead view.

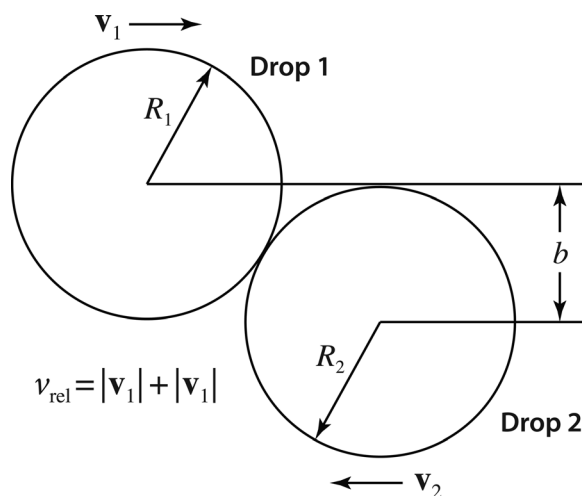


Fig. 2. Definition of the impact parameter b and other collision parameters.

Table I. Parts list.

One or more Gorman-Rupp™ oscillating pumps (model #14925-005)
Glass or plastic nozzles (straight eye-dropper type or similar to form spherical drops)
Vinyl tubing (or similar); 0.25–0.5 in inner diameter
Halogen floor lamps (500 W each)
Variable-rate strobe
Surface-tension ring and balance
Water- and oil-soluble dyes (optional; available from Bright Dyes, Miamisburg, OH 453542 and other suppliers of leak-tracing dyes)
Fluorescence (optional)
High-speed digital video recorder, preferably with time-stamped frames available.
High-resolution 35-mm digital camera (optional)
Image analysis program (NIH Image, Video Graph,™ Logger Pro,™ or similar)

uniform ≈ 60 -Hz pulsating action that, together with an appropriate nozzle, yields a reproducible stream of similar-size drops. As noted, typical drop diameters ranged from 3–8 mm with impact parameters from $b=0$ (head on) to $b=7$ mm (grazing collision between the largest drops). A list of specific parts used in the basic apparatus is given in Table I, but any similar set of components should work.

The data shown utilized a 3-CCD Sony DCR-VX1000 video camera for most of the recordings, but most modern high-speed digital video cameras will suffice. The camera is shown in the position used for side-view images [Fig. 1(b)] to determine the relevant collision parameters (Fig. 2) while the camera for top view images was placed directly above the collision point (not shown). While a good 35 mm or digital still camera with a strobe light can be used to photograph the collisions, detailed analysis from such photographs can be difficult. Therefore, we instead used the digital video camera together with high-intensity halogen lamps and stroboscopic lighting with an adjustable strobe rate to obtain frame-by-frame digital video recordings of the collisions in real time. In early measurements, uranine was often added to the water to increase visibility. Later measurements used pure liquids with the drops recorded against contrasting backgrounds with various colored screens used to enhance the video image quality or to facilitate measurements of various dimensions. The camera employed records directly in DV format with precise time-coded frame information which permits accurate frame-by-frame analysis using Apple Quicktime Video Player (or similar programs).

Individual students were encouraged to make changes in the original setup to accommodate different types of experiments. Thus, students made improvements to the nozzle arrangement or the nozzle alignment system. Another student set up two separate liquid streams, two pumps, and two reservoirs to study collisions with drops of contrasting colors. Another devised a drop-charging system by adding thin (5 mil) wires to glass nozzles and connecting these to a low-current high-voltage power supply (5–35 kV) to study collisions of charged drops. The wires were adjusted to intercept the drops at right angles after they exited the nozzle. This, and the fact that the wire was thin enough to bend as the drop passed by, caused minimal disruption of the drop. Owing to their high dielectric strength even at the highest voltage (35 kV), very little charge could be transferred to the

oil drops as evidenced by the low current output of the power supply. In contrast, the water and water-glycerine drops could be highly charged. In the case of water drops, this often led to major distortions and fragmentation of the drops even before colliding. The water-glycerine drops allowed for charging without major disruptions and made it possible to simulate several interesting phenomena.

Several of the video sequences obtained by students are available as supplementary material.³⁴

III. EXPERIMENTAL PROCEDURES AND ANALYSIS

Prior to taking digital video images, several key properties of the liquids must be determined by the students so they can better understand and characterize specific types of collisions. Thus, viscosity measurements are needed, here found by dropping marbles down a tall, large-diameter cylinder filled with the liquid. The path of the marbles is filmed by the digital camera, and the terminal velocity is calculated from analysis of the images. The viscosity then can be found from Stokes' law¹³ for the retarding force of a viscous fluid which results in a terminal velocity v_t given by

$$v_t = 2r^2g(\rho - \rho')/9\eta, \quad (1)$$

where r is the radius of the marble, $g = 9.8 \text{ m/s}^2$ is the gravitational field strength, ρ and ρ' are the densities of the marble and the liquid, respectively, and η is the viscosity.

Next, the surface tension σ for the liquids can be determined by placing a metal ring on the surface of the liquid and finding the force F required to lift it out (Fig. 3). The force needed is measured using a balance, and the surface tension is calculated using $\sigma = F/2C$, where C is the circumference of the ring. (Special surface-tension balances with suitable rings are available from many science-equipment vendors.)

While the above measurements are useful for illustrating the properties of various liquids such as vegetable oil and water, as well as demonstrating the techniques used to measure viscosity and surface tension of liquids, accurate results are often difficult to obtain. Hence, where available, the published viscosity and surface tension values were adopted for use in calculations involving water and oil.³⁵ However, values of ρ , η , and σ for water-glycerine solutions and other mixtures typically must be deduced from direct measurements and normalized, as needed, to the known, limiting cases of pure water and pure glycerine (chemical name glycerol).³⁵

The physical properties at room temperature ($T = 20\text{--}22^\circ\text{C}$) of some of the liquids used are summarized in Table II. Once the physical properties of the liquids were determined, a variety of experiments were then carried out by the students. The size (radius), mass, impact parameter, and velocities of the drops were obtained from video analysis of the collisions and the Weber and Reynolds numbers determined (see below). The latter were altered primarily by the use of the different fluids as the drop sizes and velocities were often similar between different collisions.

If a known distance and reference length (in pixels) are shown in the video frames along with the drops, the appropriate length scales can then be determined. As an example, from the known nozzle-to-nozzle distances, or a suitable grid included in the DV frames as a reference, it was determined



Fig. 3. Top: A student measuring force to determine surface tension of a liquid. Bottom: Close up of ring apparatus used to measure surface tension of a fluid.

that typically there were 17.09 pixels per cm for the oil-drop images and 5.66 pixels per centimeter for the water-based drop images. Individual drop sizes and masses could then be calculated using these calibrations. The horizontal and vertical drop velocities and the relative closing velocity V_{rel} between the drops could then be deduced from the distances traveled between the drops in successive video frames or a known set of frames using the frame-rate timing of the DV camera or other timing information (such as the 60-Hz pulse rate of the pumps and the strobe-light frequency). Typical horizontal and vertical drop velocities were in the range 20–120 cm/s and 40–130 cm/s, respectively, while closing velocities ranged from 50 to 220 cm/s, with oil at the low end and water at the high end of values. The accuracy of the

Table II. Physical properties of the fluids studied.

Liquid	ρ (g/cm ³)	η (10 ⁻³ Pa-s)	σ (10 ⁻³ N/m)
Water	1.0	1.0	72.8
Water with glycerine	1.0–1.3	4–256	42–73
Water with Photoflo™	~1	~1	31
Vegetable oil	0.92	69	84.4

parameters measured or calculated by the students with a few exceptions typically was 5%–10%.

Collisions between drops and other fluid systems can generally be characterized by four parameters: the impact parameter (b), the Weber number (We), the Reynolds number (Re), and some critical dimension parameter. In the case of colliding drops, the latter is the ratio of the colliding drop diameters (Δ).^{7,13,26–28} The Weber number for drops of similar size is calculated using the relation

$$We = \rho v^2 d / \sigma, \quad (2)$$

where ρ is the liquid density, d is the drop diameter, v ($=V_{\text{rel}}$) is the closing velocity of the drops, and σ is the surface tension. (Note that the viscosity does not appear in the Weber number). The Reynolds number, which indicates the transition between laminar and turbulent flow, is defined by¹³

$$Re = \rho v d / \eta, \quad (3)$$

where ρ is the density, d is the drop diameter, v is again the closing velocity between the drops, and η is the viscosity. (Note that the surface tension does not appear in the Reynolds number.). Other dimensionless parameters,¹³ such as the Ohnesorge parameter ($\eta / \sqrt{\rho \sigma d} = \sqrt{We/Re}$), which is a measure of the viscous dissipation expected for a specific fluid, may also be relevant but we did not study this in detail.

In the collision of drops of different diameters, it is customary to use the diameter of the smaller drop in calculating the Weber and Reynolds numbers.^{26–28} The impact parameter b describes the centrality of the collision and is graphically shown in Fig. 2, where $b=0$ for central collisions and $b=d/2$ for exactly grazing collisions. Typical collision parameters for some of the collisions studied by students are summarized in Table III. While the values determined were typically only accurate to 5%–10%, and hence less accurate than the data published in research journals, they allowed students to characterize the collisions well enough to verify some of the critical aspects of the collisions, and in particular, verify the significance of the Weber parameter and the associated impact parameter.

When considering the outcome of collisions between liquid drops, Ashgriz and Poo⁷ concluded that the Reynolds number, in contrast to fluid flow, *does not* play a significant role. The Weber number and impact parameter b , however, *do* play a major role. As an example, the boundary between coalescence and fragmentation of colliding drops often can be defined strictly in terms of the Weber number and the impact parameter. Ashgriz and Poo⁷ and Menchaca-Rocha *et al.*²⁷ demonstrated that for many systems a Weber number between 7 and 20 (depending on impact parameter) typically marks the boundary between separation and permanent coalescence for grazing-type collisions, while a higher Weber number determines the boundary for non-grazing collisions.

Table III. Typical Collision Parameters.

Liquid	Weber number	Reynolds number	Δ
Water incl. water with Photoflo	3–309	1,000–10,340	0.4–1.0
Water with glycerine	18–63	65–980	0.7–1.0
Vegetable oil	7–123	21–250	0.4–1.0

Students found, in general, that the Weber numbers for oil are very close to these boundaries. Most water drop collisions, and many of the water-glycerine drop mixtures, however, lie in the region of fragmentation.

As noted, many physics-related phenomena such as nuclear collisions may resemble colliding fluids (colliding drops). Yet few texts on fluid dynamics introduce, let alone discuss, the implications of the Weber number. Most emphasize the importance of the Reynolds number, which determines the characteristics of fluid flow, yet seems to have less importance for characterizing colliding fluids and drops, in particular. Instead, in drop collisions the Reynolds number (via the viscosity) mainly appears to affect drop formation, drop excitations, and the exact type of fragmentation, rather than determining the characteristics of the actual collision. Thus it may enter well after the collision in predicting the ultimate fate of the drops and the characteristics of any fragmentation that occurs, but it does not *a priori* determine if fragmentation will occur.²⁷ Hence the oil-drop collisions described below involve relatively low Reynolds numbers (21–250) while the water-drop collisions involved high Reynolds numbers (1,000–10,340), with water-glycerine values intermediate to both (Table III). However, the Weber numbers and impact parameters spanned similar ranges in all cases (Table III) and determine if fragmentation will occur.

IV. SELECTED RESULTS AND DISCUSSION

A. High-viscosity systems: Oil drops

Figures 4–6 illustrate a pulsed flow of oil separating into spherical drops, which then collide as they travel through the air. The collision point is chosen to be sufficiently far downstream to ensure that the drops have fully separated from each other, and also that any oscillations of the drops are mostly damped out. This is analogous to nuclei colliding in their ground states rather than in excited states. In this case, the amount of energy in the oscillations is far less than the drops' kinetic energy and should not significantly change the basic features of the collisions. The oscillations themselves are of interest as they illustrate the various excitation modes of a nucleus, mainly quadrupole oscillations. Unlike monopole (breathing mode) and dipole oscillations, this mode conserves volume as appropriate for an incompressible fluid.

The typical shape evolution for collisions between oil drops (soybean or canola vegetable oil) with impact parameter b close to zero (central collisions) is shown in the left side of Fig. 4. The data were obtained by extracting images from various DV frames for collisions between similar-size drops. It can be seen that as the drops touch, their relative incompressibility forces the liquid along the contact plane to squeeze outward. Eventually, each collision results in the



Fig. 4. Left: Shape evolution of head-on collision ($b=0$) of equal size oil drops ~ 6 mm in diameter with $We \sim 10$ (see Tables II and III). Right: same as the left panel but for a grazing collision ($b > 0$) with $We \sim 100$. Also, see videos available as supplementary material (Ref. 34).



Fig. 5. Oil drop collisions with unequal size drops ~ 4 and 6 mm in diameter with $We \sim 20$ (see Tables II and III). Left: head-on collision ($b=0$); Right: grazing collisions ($b > 0$). Also, see videos available as supplementary material (Ref. 34).



Fig. 6. Grazing collision of unequal-size colored oil drops with $We \sim 20$; the orange drop has diameter ~ 3 mm and the blue drop has diameter ~ 5 mm. Also, see the videos available as supplementary material (Ref. 34).

formation of a thin sheet of liquid with a slightly thicker border. They stay virtually unchanged for lengths of time that are long in comparison to the time frame for the actual formation of the sheet, suggesting that they are quite stable. These sheets can be seen to form after the initial collisions as shown in the video frames in the figures. The sheets often then coalesce into a drop, which represents the final state in each collision; no further fragmentation is observed before the drops hit the reservoir.

Theoretical models suggest that the formation of tori in central collisions including nuclear collisions also should be possible.²⁹ However, Menchaca-Rocha *et al.*^{26–28} reported that, among thousands of collisions observed with their apparatus, not a single torus was observed. This is in agreement with the findings here. Students were unable to observe any tori among the hundreds of liquid-drop collisions that were analyzed. This is unfortunate as it suggests that toroidal nuclei probably are unlikely to be formed in nuclear collisions. Such an exotic nuclear shape would be of considerable interest.²⁹

Images were also taken of oil drops for impact parameters close to $b = d/2$ corresponding to grazing collisions (right side, Fig. 4). This type of collision was described by Ashgriz and Poo⁷ as resulting in “stretching separation.” After the collision, the two drops form a rotating dumb-bell shape. Adam *et al.*⁸ described the stability of this dumb-bell shape to be dependent upon the rotational energy as the shape rotates about its center of mass. However, Ashgriz and Poo⁷ argued that the rotational force was negligible in comparison

with the stretching force. Thus, the dumb-bell would separate into two fragments (fission) before any significant rotation occurred. Unfortunately, due to the size limitations of the present apparatus, we were unable to observe the fragmentation of this shape. However, it appears that significant stretching is occurring, and that significant rotation is rare and only occurs with the present apparatus if the nozzles are misaligned. This appears to be consistent with the findings of Ashgriz and Poo and others.^{7–9,26–28} Nuclear collisions of this type routinely are observed with heavy nuclei and generally result in symmetric fission.

Head-on and grazing collisions involving drops, including colored drops, of unequal size ($\Delta \neq 1$) and various Weber numbers and impact parameters are shown in Figs. 5–6. Again these exhibit interesting features paralleling many of the observations noted above, but now extended to include asymmetric stretching modes for grazing collisions.

B. Low-viscosity systems: Water drops

Figures 7 and 8 illustrate a pulsed flow of water separating into spherical drops, which then collide as the drops travel through the air. The water drops aren’t quite as spherical as the oil drops, and especially notable is the formation of satellite drops as the water pulses separate from each other. The water drops notably also are less uniform, which limits the analysis of the shape evolution of the collisions.



Fig. 7. Shape evolution for water-drop collisions (see Tables II and III) for unequal size drops ~ 4 and 7 mm in diameter for various impact parameters: (left) $We \sim 15$; (center) $We \sim 80$; (right) $We \sim 250$. Also, see the videos available as supplementary material (Ref. 34).

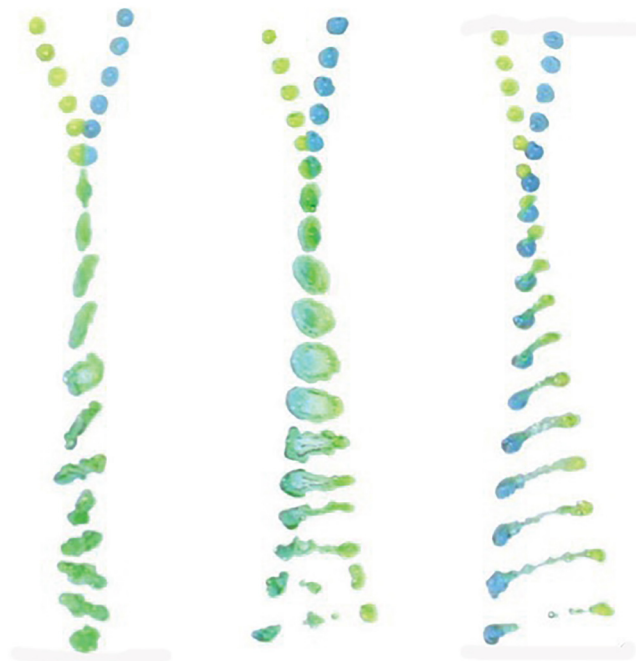


Fig. 8. Collisions of colored water drops (yellow diameter ~ 4 mm, blue diameter ~ 6 mm): (left) head-on, $We \sim 20$ to (right) grazing $We \sim 60$. The videos available as supplementary material (Ref. 34) show the mass transfer between the drops in more detail.

However, some interesting qualitative observations of these collisions can be made. Some typical images of central collisions (b near zero) between water drops are included in the left-side images shown in Figs. 7 and 8. These images clearly show that sheet formation occurs for collisions between water drops at high velocities. These sheets are significantly less stable than the sheets produced in the oil-drop collisions and often are produced along with a high number of smaller satellite drops. Fragmentation along the border can be seen almost immediately after the sheets are formed (see Figs. 7 and 8). Close-up photos taken with a high-resolution 35 mm digital camera³⁴ often display features, although usually to a lesser degree, of what Menchaca-Rocha *et al.* call the “Mexican hat” instability.^{26–28} This instability occurs at the beginning of the fragmentation process with Weber number near or above 20, when the slightly thicker rim that borders the sheet begins to develop fingers. These fingers can lead to the development of many smaller drops as the sheet disintegrates, and resembles the classic milk-drop stroboscopic photos of Edgerton.^{1,2}

Likewise, grazing collisions were observed for water drops where the impact parameter is near or at $b = d/2$. Some typical images are shown in the right and central panels of Figs. 7 and 8. These collisions exhibit the same general shape that was observed for the oil drops with $b = d/2$, however, the neck is undergoing a twisting motion that was not evident in oil-drop collisions and quickly fragments. The latter produces numerous satellite drops that often have formed around the dumbbell, and the edges of the remaining drops are exhibiting a fingering instability.

The DV data show many collisions where the neck of the dumbbell has completely shattered. It is interesting to note that this violent fragmentation almost always results in two large drops with masses comparable to the original drops, along with many small “satellite” drops. Other data on

colliding water drops may be found in Refs. 6–9 in the context of the formation and coalescence of raindrops, for example.

As expected, adding a wetting agent (Kodak Photoflo or equivalent) to the drops will greatly reduce the surface tension, raise the Weber number, and lead to highly fragmented, rather chaotic collisions. The latter resemble many of the galactic collisions that have recently been observed using the Hubble space telescope and the new generation of land-based large-aperture telescopes (see Fig. 9).

C. Water-glycerine drops

It is possible to systematically change, over a wide range, the properties of water-based drops by the addition of various amounts of glycerine (chemical name glycerol). This alters the surface tension and increases the viscosity and thus permits one to simulate features of a liquid intermediate to water and oil. Likewise other collision parameters can be altered to span a wide range of corresponding Weber and Reynolds numbers, from $We = 18$ to 63 and $Re = 65$ to 980 in some of the experiments (Table III). As anticipated, the collisions (some shown as charged drops) qualitatively are as expected based on the Weber number of the liquid and the impact parameters. This confirms the important role played by those in describing the collisions, or the transition between coalescence and fragmentation at high Weber numbers (above or near 20 for grazing collisions).

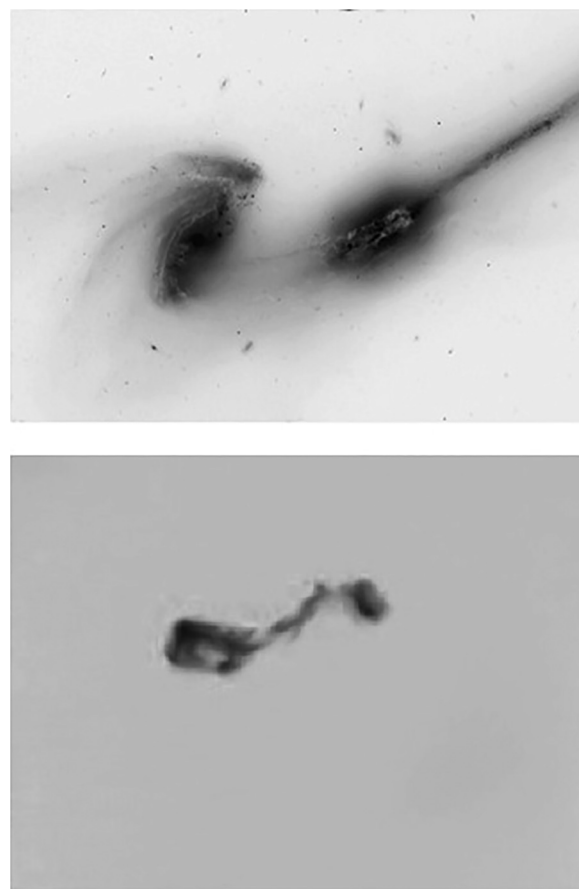


Fig. 9. Comparison of images of the colliding Mice galaxies NGC44676 (top; NASA-HST photo) and of two colliding water drops with $We > 100$ (bottom). Also, see the videos available as supplementary material (Ref. 34).

However, as noted, the Reynolds number also appears to play a role (via the viscosity) in describing the pre- and post-collision drop shapes, excitations, and ultimate type of fragmentation. This was apparent when a smaller drop collided with a larger drop ($\Delta \neq 1$, see Figs. 5–7). Over a fairly wide range of impact parameters, one or more small moon-like droplets are often formed. This illustrates the type of collision thought to be responsible for forming the Earth’s moon and other moons surrounding planets in our and similar solar systems.

D. Observing mass transfer in collisions of colored drops

As mentioned earlier, a subset of the collisions studied by one particular student utilized drops of contrasting colors



Fig. 10. Near head-on collision of charged oil drops, diameter ~ 6 μm ($V = 35$ kV). Also, see the videos available as supplementary material (Ref. 34).

using the modified setup described in Sec. II. Selected data are shown in Figs. 6 and 8, where one can now observe the transfer of fluid (mass) between the drops during a collision. In the case of head-on collisions that coalesce, there is significant mixing of the two fluids, while for grazing collisions there only is partial mixing even though the drops on closer inspection appear to interpenetrate during the collision. Some other unusual features were observed in the bridging parts between drops where different colored fluids from the original drops appeared to oscillate across the liquid bridge formed between the drops. It would be interesting to see if there are nuclear analogs of this phenomena.

E. Observations with charged drops

In order to better illustrate the features of nuclear collisions, a student developed an apparatus for charging the drops. Various water-glycerine drops were made positively charged, their collisions recorded and then studied. Typical collision data are shown in Fig. 10 (with additional material available³⁴). Charging the drops makes a normal fusion collision (one with low Weber number) become unstable and lead to fission, thus changing the collision dynamics. However, unlike a nucleus, the charge on the drop is mostly on the surface (rather than throughout the volume) and the forces involved are molecular rather than nuclear. Yet by charging the drops, as well as varying the impact parameter and closing velocities, it was possible to illustrate an important type of nuclear collision: fusion followed by fission. The drop collisions of this type show considerable necking during the last stages of the collision and usually results in formation of one or more small droplets between the fragments (see Fig. 10). This is analogous to the formation of one or more small nuclear fragments during nuclear fusion-fission, and in particular, due to their extra stability, alpha particles. The alpha particles in such a nuclear process would then be accelerated with emission at right angles to the large, separating, co-linear, high- Z , positively charged fission fragments. This unusual type of nuclear fission (tertiary fission with formation and emission of an energetic alpha particle), although rare, has been observed.²⁰

V. CONCLUSIONS

Collisions between oil, water, and water-glycerine drops have been studied by students using a relatively simple colliding-drop apparatus suitable for use in a formal laboratory, as part of independent research projects (as the case here), or for use as a class demonstration. Oil-drop collisions and many water-glycerine drop collisions have a low Weber number, and therefore, depending on impact parameter are often observed to lie in the region of coalescence. The results for these collisions parallel many of the experimental findings of Menchaca-Rocha *et al.*,^{26–28} and also appear to support many of the conclusions reached by Ashgriz and Poo, and others^{7–9} concerning the importance of stretching forces versus rotational forces. The collisions of oil and certain water-glycerine drops often resemble many of the features seen in various types of nuclear collisions, including fusion followed by fission. Such collisions also appear to resemble features seen in calculations of the initial stages of collisions between *very* large nuclei, such as neutron stars (see the Appendix). The latter are candidates as the source of certain

types of intense extra-galactic γ -ray bursts recently observed and hence are of great interest in astrophysics.

Water and certain water-glycerine drop collisions have a substantially higher Weber number and generally undergo fragmentation. The collision is violent and chaotic in the case of pure water or water with a wetting agent added. To date, no rigorous analysis of shattering collisions has been published so it was not possible to make any comparisons with existing data. However, students observed some interesting characteristics of these collisions. In particular, the central water-drop collisions (b near zero) often exhibit features of the “Mexican hat” instability seen by others, and the grazing collisions exhibit some interesting characteristics as well. Again, a systematic analysis of the shattering phenomenon for high Weber number collisions was beyond the scope of our studies; however, the observations suggest that there is a great deal to be learned by studying these collisions. In particular, the collisions of water and water-glycerine drops appear to exhibit features similar to those of colliding galaxies, as seen using the Hubble space telescope (see the [Appendix](#)).

Data also were obtained using colored drops to study the mass transfer between the drops during a collision. Likewise, limited data were obtained with charged drops. Both of these exhibit some interesting features and would warrant further study. Specifically, the use of colored drops and a suitable video analysis of the color mixing of the liquids during a collision could provide a method to track the mass transfer between drops during the collisions. This could prove especially interesting as it appears modern computer simulations can be performed for such data^{48–50} and there may be analogous phenomena that could be observed in nuclear collisions.

There are a number of improvements or changes that could be made to the present apparatus, such as more nozzle sizes or variable nozzles (to vary drop size over a wider range), more precise nozzle movement (to more easily change impact parameters), add provisions for two colliding liquids having very different properties or relative velocities, providing modifications for study of drop collisions with surrounding low (or high) pressure,⁵¹ and incorporating modifications to generate and study collisions of gas bubbles emerged in various liquids. These again could serve as interesting and highly educational undergraduate research projects. In any case, the study of liquid-drop collisions and similar phenomena involving liquids, although often utilizing simple apparatus as is the case here, continues to be an active, fore-front research area (e.g., see Ref. 52 and related references therein).

ACKNOWLEDGMENTS

The authors thank M. Y. Lee, T. O'Donnell, D. Allen, J. Pluta, M. Shapiro, D. Roberts, A. Gambino, M. Ratajczak, the late Professor H. R. Crane, and Professor F. Adams, Professor G. Evrard, Professor K. Thornton, and Professor G. Holt for their help. The authors also thank the referees for providing several useful suggestions that were incorporated into the final version of the paper. Early versions of the apparatus, data, and video collision analysis were described at an AAPT meeting.⁵³ This work was supported in part by the U.S. National Science Foundation Grant Nos. PHY-9512104, PHY-9804869, and PHY-0969456. Three of the authors (S.L.M., W.R.R., and M.O.) were supported by

various NSF Research Experience for Undergraduates (REU) grants.

APPENDIX: BACKGROUND MATERIAL

In this [Appendix](#), we provide additional details, tutorial material, and references for some of the underlying physics related to some of the specific collisions illustrated with the colliding-drop apparatus.

1. Nuclear fusion-fission and the LDM

The balance between the volume-, surface-, and Coulomb-energy terms in the nuclear LDM^{11,19} sets a basic limit on the maximum size or volume to surface ratio, and charge (Z) for a stable nucleus (we exclude neutron stars; see below). Thus, nuclei with $A > 240$ and $Z > 94$ are generally unstable and may undergo spontaneous fission or α -particle decay as these processes yield two or more nuclei lower in total mass.^{15–24} Likewise, colliding nuclei that have coalesced to a system near or beyond this limit also will fission via a fusion followed by a fission process (“fusion-fission”).²⁰ Fission generally will be enhanced when there is some rotational energy in the system to facilitate the transition through the fission barrier.²⁰ In oil-drop collisions, the latter corresponds to grazing collisions and indeed fusion-fission is the primary collision mode when $b > 0$. This is quite fortuitous as one spans a distance scale of about 10^{10} (10^{-4} m for drops vs 10^{-14} m for nuclei). Even modest excitation of a heavy nucleus near the limit of fission stability will usually cause the system to fission with a large, net release of energy. Even the great physicist, Bohr, who had developed much of the nuclear LDM formalism,¹⁷ did not recognize this until Meitner and Hahn discovered nuclear fission in 1939.^{15,16}

Another form of fission, again predicted by the LDM and verified experimentally by Petrzhak and Flerov in 1940, is the long-lived, *spontaneous* fission of nuclei at the limits of fission stability.²² Man-made, short-lived spontaneous fission sources such as ²⁵²Cf are well-suited for study of this process (and the LDM) in an advanced undergraduate laboratory.²⁴

2. Nuclear fragmentation and the quark-gluon plasma

At high kinetic energies and densities (for large We) one expects, and indeed observes, that multi-particle fragmentation is the primary feature of most nuclear collisions, especially for head-on collisions ($b = 0$). In the collision of oil and other dense liquids under these conditions, we and others^{26–28} often observe the production of many small droplets. In a high-energy nuclear collision, this can correspond to the emission of α -particles and nucleons (n, p, \dots) or even sub-nuclear fragments (various mesons, etc.). At sufficiently large kinetic energy, central nucleus-nucleus collisions ($b = 0$ and relativistic) may cross the threshold needed to produce quark-gluon droplets in the quark-gluon phase of nuclear matter. The Relativistic Heavy-Ion Collider (RHIC) at Brookhaven National Laboratory (New York, USA) is specifically designed to study this type of collision. Recent data at RHIC for collisions of GeV/nucleon lead on lead nuclei seem to indicate that such a state similar to a quark-gluon plasma has been observed.^{25,36} At these high collision

energies, the nuclear matter formed is highly heated and both the surface tension and viscosity drops dramatically as the quark-gluon plasma is formed.

3. The LDM, neutron stars, and γ -ray bursters (GRB)

One of the most unusual predictions of the LDM is the existence of a special type of *very* large yet stable “nucleus” of neutrons with a diameter of a few kilometers! This prediction was formulated in detail by Oppenheimer and others in the 1930s,³⁷ where they examined the consequences of adding the gravitational-energy term to the nuclear LDM. Since this term for sufficiently large nuclei (mass \approx mass of the sun) can be comparable to the nuclear-energy terms, the possibility of unusual types of stable *macroscopic* nuclear systems appeared possible.^{37–39} It was further predicted that at high gravitational energy (and hence pressure) nuclear protons would convert to neutrons which would lead to a stable, but *very large* macroscopic nuclear system known as a neutron star. Such objects were considered to be theoretical oddities until pulsars were discovered in the 1960s.⁴⁰ The latter owing to their short (typically ms) radio pulsations are identified as compact, rotating neutron stars,^{40,41} as had been predicted from the LDM.

Although rare, two neutron stars, which are considered to be remnants of super-nova explosions, have some small but finite probability of colliding on galactic time scales. Recently, several sources of intense X- and γ -radiation bursts, thought to be exceeded in energy released only by the Big Bang itself, have been located. The optical flash associated with a specific X- and γ -ray bursters (GRBs) has been identified with distant extra-galactic sources.⁴² It has been speculated that such energetic processes are likely the result of colliding neutron stars, at least for a certain class of GRBs. A collision of neutron stars, again owing to the low effective Weber number for media involving nuclear matter, might be expected to initially resemble a collision between oil drops with the effects of strong gravitational attraction now added between the drops. While calculations suggest that the initial collision process and subsequent fusion resembles that of oil drops and colliding nuclei, like all astrophysical collisions gravity plays a dominant role after the initial collision. Whereas nuclei will first fuse and then fission (due to Coulomb repulsion), fragments of colliding neutron stars instead will try to coalesce after the initial encounter. The time evolution of the emitted radiation during the collision can provide information on the time scale for coalescence. This also is the case for colliding galaxies.

4. Colliding galaxies, star clusters, and asteroids

Galaxies have certain characteristics in common with those of water and/or certain water-glycerine drops in that the gravitational binding energy of galaxies acts like a volume energy term and hence, produces viscosity. The effective galactic surface tension is low as the interaction between galactic constituents (stars) is long range (gravity) and there is little or no apparent surface tension *per se*.^{43–46} Because the equivalent surface tension is low, the effective Weber number for a galactic collision [Eq. (2)] can be very large, implying that collisions between galaxies often should resemble collisions between water drops in non-coalescing collisions (with certain water-glycerine or water-wetting agent mixtures). Indeed, recent numerical simulations and

the limited amount of observational data appear to support this picture,^{43–46} especially the bridging and tailing that we also observe in many water-drop collisions (see Fig. 9).

Galaxies are not incompressible fluids of course (they more closely resemble a gas), and they often contain large amounts of rotational energy as well as gravitational energy.⁴⁷ Nonetheless, LDM collision parameters, and the Weber number, in particular, appear to be useful entities and can provide insight for understanding the features of galactic collisions. Again, as in the case of colliding neutron stars, gravitational attraction will cause the system to at least partially coalesce after the initial collision. This is thought to be responsible for many of the unusual galactic shapes often observed, such as the Antenna and Mice galaxies, and similar galactic systems.^{44,45} It also is interesting to note that many galaxies, if not most (including our own Milky Way), are likely the result of past galactic collisions. Many are yet again on a collision path with nearby galaxies; in the case of our galaxy a collision with the Andromeda galaxy.⁴⁶ Also, the formation of the planets and our moon are thought to be the result of collisions involving asteroids,⁴⁷ so these can be expected to resemble certain liquid-drop collisions with highly viscous constituents.

The above all illustrate some of the interesting physics phenomena that can be illustrated with the simple colliding-drop apparatus described here. This can serve to encourage students to pursue further study in these areas, as many of the students involved with this project have done.

^aElectronic mail: fdb@umich.edu

^bPresent address: Center for Coastal Physical Oceanography, Old Dominion University, Norfolk, Virginia 23529.

^cPresent address: Department of Physics, North Carolina State University, Raleigh, North Carolina 27695.

^dPresent address: Department of Homeland Security, Washington, DC 20528.

¹Harold E. Edgerton, *Electronic Flash, Strobe*, 3rd ed. (The MIT Press, Cambridge, Massachusetts, 1992).

²Harold E. Edgerton and James R. Killian, Jr., *Moments of Vision: The Stroboscopic Revolution in Photography* (The MIT Press, Cambridge, Massachusetts, 1984), pp. 18–31.

³Walter Wick, *A Drop of Water* (Scholastic Press, New York, 1997).

⁴Sidney R. Nagel, “Klopsteg memorial lecture (August, 1998): Physics at the breakfast table or waking up to physics,” *Am. J. Phys.* **67**(1), 17–25 (1999).

⁵Jens Eggert, “Non-linear dynamics and breakup of free-surface flows,” *Rev. Mod. Phys.* **69**, 865–929 (1997).

⁶H. T. Ochs III, R. R. Czys, and K. V. Beard, “Laboratory measurement of coalescence efficiencies for small precipitation drops,” *J. Atmos. Sci.* **43**, 225–232 (1986).

⁷N. Ashgriz and J. Y. Poo, “Coalescence and separation in binary collisions of liquid drops,” *J. Fluid Mech.* **221**, 183–204 (1990).

⁸J. R. Adam, N. R. Lindblad, and C. D. Hendricks, “The collision, coalescence and disruption of water droplets,” *J. Appl. Phys.* **39**(11), 5173–5180 (1968).

⁹J. Qian and C. K. Law, “Regimes of coalescence and separation in droplet collision,” *J. Fluid Mech.* **331**, 59–80 (1997).

¹⁰G. Smedley, “Preliminary drop-tower experiments on liquid-interface geometry in partially filled containers at zero gravity,” *Exp. Fluids* **8**, 312–318 (1990); see also <<http://quest.nasa.gov/smores/background/micro-gravity/MGintro3.html>>.

¹¹C. F. von Weizsacker, “Theory of nuclear masses,” *Z. Phys.* **96**(7–8), 431–458 (1935).

¹²N. Bohr, “Neutron capture and nuclear constitution,” *Nature* **137**(3461), 344–348 (1936).

¹³Bruce R. Munson, Donald F. Young, Theodore H. Okiishi, and Wade W. Huebsch, *Fundamentals of Fluid Mechanics*, 7th ed. (John Wiley, Hoboken, N.J. 2013), Sect. 7.6; R. V. Giles, J. B. Evett, and Cheng Liu, *Schaum’s Outline of Theory and Problems of Fluid Mechanics and*

- Hydraulics*, 3rd ed. (Schaum's Outline Series, McGraw-Hill, Inc., N.Y., N.Y. 1998), Chap. 6.
- ¹⁴W. D. Myers, *Droplet Model of Atomic Nuclei* (Plenum, New York, 1977).
- ¹⁵L. Meitner and O. R. Frisch, "Disintegration of uranium by neutrons: a new type of nuclear reaction," *Nature* **143**, 239–240 (1939); "Products of the fission of the uranium nucleus," *ibid* **143**, 471–472 (1939).
- ¹⁶O. Hahn, "The discovery of fission," *Sci. Am.* **198**(2), 76–84 (1958).
- ¹⁷N. Bohr and J. A. Wheeler, "Mechanism of nuclear fission," *Phys. Rev.* **56**, 426–450 (1939).
- ¹⁸E. K. Hyde, *The Nuclear Properties of the Heavy Elements* (Prentice-Hall, Engelwood Cliffs, NJ, 1964), Vols. I–III.
- ¹⁹John Lilley, *Nuclear Physics* (J. Wiley, NY, 2001) Chapt. 2.
- ²⁰R. Vandenbosch and J. R. Huizenga, *Nuclear Fission* (Academic Press, N.Y., N.Y., 1973) and references cited there.
- ²¹V. M. Strutinsky, "Shell effects in nuclear masses and deformation energies," *Nucl. Phys. A* **95**, 420–442 (1967); **122**, 1–33 (1968).
- ²²K. A. Petrzhak and G. N. Flerov, "Spontaneous fission of uranium," *Sov. J. Phys.* **10**, 1013–1017 (1940).
- ²³W. Swiatecki, "Systematics of fission asymmetry," *Phys. Rev.* **100**, 936–937 (1955); "Systematics of fission thresholds," *ibid.* **101**, 97–99 (1956).
- ²⁴F. D. Becchetti and J. S. Ying, "Student experiments in spontaneous fission," *Am. J. Phys.* **49**(12), 1162–1171 (1981).
- ²⁵A. Szanto de Toledo *et al.*, "Are hot light nuclei liquid droplets?," *Phys. Rev. Lett.* **70**(14), 2070–2073 (1993).
- ²⁶A. Menchaca-Rocha, A. Cuevas, M. Chapa, and M. Silva, "Rotating-liquid-drop model limit tested on macroscopic drops," *Phys. Rev. E* **47**(2), 1433–1436 (1993).
- ²⁷A. Menchaca-Rocha, F. Huidobro, A. Martinez-Davalos, K. Michaelian, A. Perez, V. Rodriguez, and N. Carjan, "Coalescence and fragmentation of colliding mercury drops," *J. Fluid Mech.* **346**, 291–318 (1997); A. Menchaca-Rocha, A. Martinez-Davalos, R. Nez, S. Popinet, and S. Zaleski, "Coalescence of liquid drops by surface tension," *Phys. Rev. E* **63**, 046309 (2001).
- ²⁸A. Menchaca-Rocha, M. Borunda, S. S. Hidalgo, F. Huidobro, K. Michaelian, and V. Rodrigues, "Search for exotic shapes in liquid-drop collisions," *Adv. Nucl. Dyn.* **2**, 299–306 (1996).
- ²⁹H. M. Xu, J. B. Natowitz, C. A. Gagliardi, R. E. Tribble, C. Y. Wong, and W. G. Lynch, "Formation and decay of toroidal and bubble nuclei and the nuclear equation of state," *Phys. Rev. C* **48**, 933–936 (1993).
- ³⁰H. R. Crane, Ann Arbor Hands-On Museum, private communication; See also Billy Tobar, "The water drop parabola," *Phys. Teach.* **18**, 371–372 (1980); A. Menchaca-Rocha, M. E. Brandan, M. Gutierrez, and R. Labbe, "Liquid drop collider to simulate nuclear reactions," *Phys. Teach.* **24**, 104–107 (1986).
- ³¹W. Rasband *et al.*, NIH Image (National Institute of Health; available from NIH website: <www.nih.gov>).
- ³²*VideoPoint*, Lenox Softworks, Lenox, MA; <<http://www.lsw.com/video-point/vp/>>.
- ³³*Logger Pro 3*, Vernier Software and Technology, Beaverton, OR; <<http://www.vernier.com/>>.
- ³⁴See supplementary material at <http://dx.doi.org/10.1119/1.4926958> for various movies, notes, and pictures.
- ³⁵*Handbook of Chemistry and Physics* (CRC Press, Boca Raton, FL, 1996), Sec. F6.
- ³⁶X. Cheng, G. Varas, D. Citron, H. M. Jaeger, and S. R. Nagel, "Collective behavior in a granular jet: Emergence of a liquid with zero surface-tension," *Phys. Rev. Lett.* **99**, 188001 (2007); see also <www.rhic.bnl.gov> and links therein.
- ³⁷J. R. Oppenheimer and G. M. Volkoff, "On massive neutron cores," *Phys. Rev.* **55**, 374–381 (1939).
- ³⁸H. A. Bethe and M. B. Johnson, "Dense baryon matter calculations with realistic potentials," *Nucl. Phys. A* **230**, 1–58 (1974).
- ³⁹W. S. C. Williams, *Nuclear and Particle Physics* (Clarendon Press, Oxford, U.K., 1990; Rev. 1996), pp. 56–65.
- ⁴⁰D. Clark, *The Quest for SS433* (Dutton Press, Hialeah, FL, 1985) and references therein.
- ⁴¹G. Greenstein, *Frozen Star* (Freundlich Books, 1984) and references therein.
- ⁴²R. Cowan, "Catching a burst's visible glow," *Sci. News* **155**, 70 (1999).
- ⁴³James Binney and Scott Tremaine, *Galactic Dynamics* (Princeton U.P., Princeton, New Jersey, 1987).
- ⁴⁴Joshua Roth, "When galaxies collide," *Sky Telesc.* **95**(3), 48–52 (1998), available on line at <http://www.shopatsky.com/sky-and-telescope-march-1998-digital-issue>.
- ⁴⁵*Paired and Interacting Galaxies*, edited by J. W. Sulentic, W. C. Keel, and C. M. Telsco, NASA Conference Publication 3098 (NASA Tech. Info. Div., Washington, D.C., 1990).
- ⁴⁶See, for example, computer simulations at <<http://www.ifa.hawaii.edu/faculty/barnes/research>>, <<http://csep10.phys.utk.edu/guidry/violence/violence-root.html>>, and <<http://www.youtube.com/watch?v=ow9JCXy1QdY>>.
- ⁴⁷Roger A. Freedman, Robert M. Geller, and William J. Kaufmann, *Universe*, 10th ed. (W. H. Freeman, N.Y., N.Y., 2013).
- ⁴⁸Alejandro Acevedo-Malav and Maximo Garca-Sucre, "Coalescence collision of liquid drops I: Off-center collisions of equal-size drops," *AIP Adv.* **1**, 032117 (2011).
- ⁴⁹Alejandro Acevedo-Malav and Maximo Garca-Sucre, "Coalescence collision of liquid drops II: Off-center collisions of unequal-size drops," *AIP Adv.* **1**, 032118 (2011).
- ⁵⁰F. Mashayek, N. Ashgriz, W. J. Minkowycz, and B. Shotorban, "Coalescence collision of liquid drops," *Int. J. Heat Mass Transfer* **46**, 77–89 (2003).
- ⁵¹A. Latka, A. Strandburg-Peshkin, M. M. Driscoll, C. S. Stevens, and S. R. Nagel, "Creation of prompt and thin-sheet splashing by varying surface roughness or increasing air pressure," *Phys. Rev. Lett.* **109**, 054501 (2012).
- ⁵²J. D. Paulsen, J. C. Burton, and S. R. Nagel, "Viscous to inertial crossover in liquid drop coalescence," *Phys. Rev. Lett.* **106**, 114501 (2011).
- ⁵³F. D. Becchetti, A. Gambino, and M. Ratajczak, *AAPT Announcer* (Summer AAPT Meeting, AAPT, College Park, MD, 2003).